

# Test of the notch technique for determining the radial sensitivity of the optical model potential<sup>\*</sup>

YANG Lei   LIN Cheng-Jian<sup>1)</sup>   JIA Hui-Ming   XU Xin-Xing   MA Nan-Ru   SUN Li-Jie   YANG Feng  
 ZHANG Huan-Qiao   LIU Zu-Hua   WANG Dong-Xi

China Institute of Atomic Energy, Department of Nuclear Physics, Beijing, 102413, China

**Abstract:** Detailed investigations on the notch technique are performed on the ideal data generated by the optical model potential parameters extracted from the  $^{16}\text{O}+^{208}\text{Pb}$  system at the laboratory energy of 129.5 MeV, to study the sensitivities of this technique on the model parameters as well as the experimental data. It is found that, for the perturbation parameters, a sufficient large reduced fraction and an appropriate small perturbation width are necessary to determine the accurate radial sensitivity; while for the potential parameters, almost no dependence was observed. For the experimental measurements, the number of data points has little influence for the heavy target system, and the relative inner information of the nuclear potential can be derived when the measurement extended to a lower cross section.

**Key words:** optical model potential; notch technique; sensitive region; elastic scattering

**PACS:** 24.10.Ht; 25.70.Bc

## 1 Introduction

The optical model potential (OMP) is the most fundamental ingredient in the study of nuclear reaction mechanism [1]. Nowadays, with the development of radioactive ion beams (RIBs), the studies of the OMPs for the weakly-bound systems have attracted particular interest, and several abnormal properties has been observed, such as the break-up threshold anomaly (BTA) [2, 3].

The OMP parameters can be extracted effectively by means of fitting the elastic scattering data. However, for a given elastic scattering angular distribution, there exists numerous different families of OMP parameters that all can give successful descriptions of the experimental data, which is the so-called Igo ambiguity [4]. It is meaningful to discuss the OMP only within the sensitive region [5], where the OMP parameters can be determined accurately by the elastic scattering. Therefore, it is quite important to know what radial regions of the nuclear potential can be well mapped by the analysis of elastic scattering data before making any discussion on the potential.

There are several ways to extract the radial region of the potential sensitivity [5–7]. The frequently-used method is to find the crossing-point radius of the potential [7, 8]. However, such a sharply-defined sensitive

radius is incompatible with the principles of quantum mechanics, and its value varies with different radial form factors adopted for the OMP [9]. Conflicting results are often brought out, e.g. the multi-crossing points [8, 10], especially for the energies close to the Coulomb barrier.

In Ref. [5], a notable technique, the notch-perturbation method was developed, which permits an intuitionistic investigation on the sensitive region of the OMP. Although the notch technique possesses evident advantages, only a few works [8, 11, 12] adopted this method to analyze the radial sensitivity of the OMP. In Refs. [5, 11], the importance of the selection of the perturbation parameters has been suggested. However, the dependence of this technique on the parameters related to the perturbation, the OMP, and the experimental measurement has not been investigated so far. In the present work, a detailed inspection on the notch technique is performed, in order to lay a more reliable foundation for extending the application of this technique.

## 2 The notch technique

The principle of the notch technique is to introduce a localized perturbation into either the real or imaginary radial potential, and move the notch radially through the potential to investigate the influence arising from this perturbation on the predicted cross section [5].

<sup>\*</sup> Supported by National Natural Science Foundation of China (Nos. 11375268, 11475263, U1432246 and U1432127) and the National Key Basic Research Program of China (No. 2013CB834404)

1) E-mail: cjlin@ciae.ac.cn

©2013 Chinese Physical Society and the Institute of High Energy Physics of the Chinese Academy of Sciences and the Institute of Modern Physics of the Chinese Academy of Sciences and IOP Publishing Ltd

The nuclear potential is defined as

$$U_N = V(r) + iW(r) = -V_0 f_V(r) - iW_0 f_W(r), \quad (1)$$

where the  $V_0$  and  $W_0$  are depths of the real and imaginary parts of the potential with Woods-Saxon form  $f_i(r, a, R)$ ,

$$f_i(r, a, R) = [1 + \exp(\frac{r - R_i}{a_i})]^{-1}, i = V, W, \quad (2)$$

where  $R_i = r_{0i}(A_P^{1/3} + A_T^{1/3})$ ,  $A_P$  and  $A_T$  represent the mass numbers of the projectile and target, respectively.

Taking the real potential  $V(r)$  as an example, the perturbation of the potential  $V_{\text{notch}}$  can be expressed as

$$V_{\text{notch}} = dV_0 f_V(R', a, R) f_{\text{notch}}(r, a', R'), \quad (3)$$

where,  $R'$  and  $a'$  represent the position and width of the notch,  $d$  is the fraction by which the potential is reduced, and  $f_{\text{notch}}(r, a', R')$  is the derivative Woods-Saxon surface form factor:

$$f_{\text{notch}}(r, a', R') = 4 \exp(\frac{r - R'}{a'}) / [1 + \exp(\frac{r - R'}{a'})]^2. \quad (4)$$

Thus the perturbed real potential  $V(r)_{\text{pert.}}$  is:

$$V(r)_{\text{pert.}} = V_0 f_V(r, a, R) - V_{\text{notch}}. \quad (5)$$

The perturbation for the imaginary potential can be derived with the same procedure. The typical perturbed potential with  $r_0 = 1.25$  fm,  $a = 0.65$  fm,  $R' = 10$  fm,  $a' = 0.1$  fm, and  $d = 1.0$  is shown in Fig. 1.

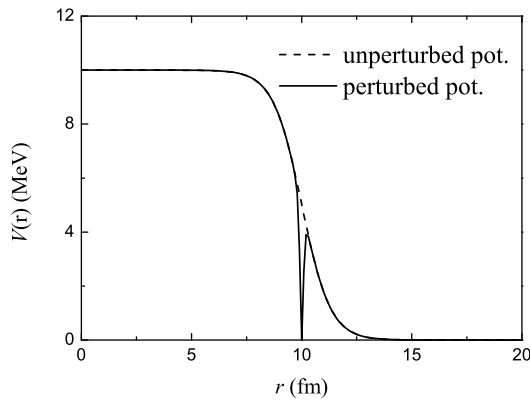


Fig. 1. The typical unperturbed potential (dashed curve) and perturbed potential (solid curve) with  $r_0 = 1.25$  fm,  $a = 0.65$  fm,  $R' = 10$  fm,  $a' = 0.1$  fm, and  $d = 1.0$ .

When the perturbation locates at the sensitive region, where the predicted cross section depends strongly on the details of the potential, the calculated elastic scattering angular distribution will change greatly. This means, when compared with the experimental data, there will

be a dramatic variation in the  $\chi^2$  value. On the contrary, at the position where the evaluated cross section is not sensitive to the potential, the perturbation has little influence on the calculated angular distribution. By means of the notch technique, the sensitive region of the nuclear potential can be presented visually and explicitly.

### 3 Sensitivity test of the notch technique

There may be several factors, from either the model parameters or the quality of the experimental data, will affect the OMP sensitivity derived from the notch technique. The influences from some possible factors will be investigated in this section, to provide a guidance on the application of the notch technique and the procedure of experiment. The code FRESKO [13] was used to perform the optical model calculations.

#### 3.1 data generation

The elastic scattering data set of  $^{16}\text{O} + ^{208}\text{Pb}$  at  $E_{\text{lab}}(^{16}\text{O}) = 129.5$  MeV [14], as shown in Fig. 2, was chosen to perform the sensitivity test. That is because this data is quite precise and measured in an extensive angle region but with small angle interval, and the ratio  $d\sigma_{\text{el}}/d\sigma_{\text{Ru}}$  was measured down to  $10^{-4}$  level. Meanwhile there is a clear picture for the interaction of this classic tightly-bound system, and the elastic scattering angular distribution can be described satisfactorily by the optical model. Moreover, at the energy well above the Coulomb barrier, the nuclear force has more significant effect on the interaction progress, which is in favor of the investigation on the radial sensitivity of nuclear potential.

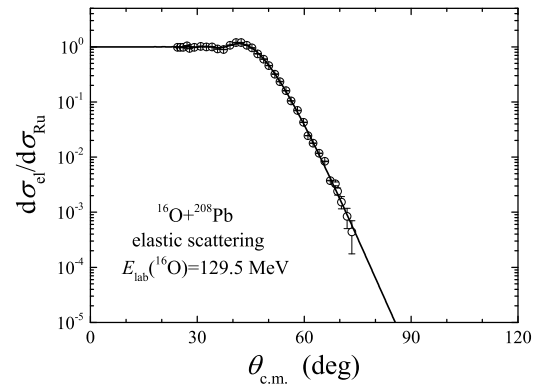


Fig. 2. Angular distributions of  $^{16}\text{O} + ^{208}\text{Pb}$  elastic scattering at  $E_{\text{lab}}(^{16}\text{O}) = 129.5$  MeV [14]. The solid curve shows the fitting result with  $V = 31.46$  MeV,  $W = 30.0$  MeV,  $r_{0i} = 1.25$  fm and  $a_i = 0.65$  fm, where  $i = V$  and  $W$ .

In order to completely eliminate the uncertainties from the experimental data, such as the statistics, angle step and range to be measured, a theoretical angular distribution was generated by fitting the experimental

data with  $r_{0i} = 1.25$  fm and  $a_i = 0.65$  fm, as the solid curve shown in Fig. 2. This theoretical data can be regarded as an ideal data set with fixed angle step of  $0.1^\circ$  and statistic error of 1%. Considering the comparability with the actual experimental situation, the theoretical data is cut off at  $\theta_{c.m.} = 80^\circ$ , where the  $d\sigma_{el}/d\sigma_{Ru}$  is down to  $10^{-5}$  level. The following calculations and discussions are based upon this equivalent angular distribution.

### 3.2 dependence on model parameters

The dependence on model parameters were investigated first, including the perturbation parameters  $d$  and  $a'$ , as well as the OMP parameters  $r_{0i}$  and  $a_i$ .

#### 3.2.1 perturbation parameters

The influence of the notch depth was investigated with the value of the reduced fraction  $d$  varied in a certain step, while the notch width  $a'$  fixed at 0.05 fm. The variations of relative  $\chi^2$  at different  $d$  values are shown in Fig. 3. It can be seen that the greater the perturbations are, the larger the relative  $\chi^2$  values will be brought. Distinct peaks are observed for both the real and imaginary parts, corresponding to the radial sensitivity regions of the nuclear potential. For the real part, a main peak lies at the position around 11.92 fm, followed by a tiny peak in the inner region around 11.0 fm. While for the imaginary part, two obvious peaks are observed: a major peak at around 12.20 fm and a minor peak at around 11.20 fm. Little changes on the sensitive region are induced by the variations of  $d$ , except for the the lowest  $d$  value 0.2. In that case, a broad peak was presented at about 11.5 fm in the imaginary part as shown in the Fig. 3(b), which is incompatible with others. It indicates that a too small reduced fraction of the perturbation may cause some spurious sensitivity region of the potential. The  $d$  value larger than 0.5 is recommended and fixed at 1.0 in the following discussions.

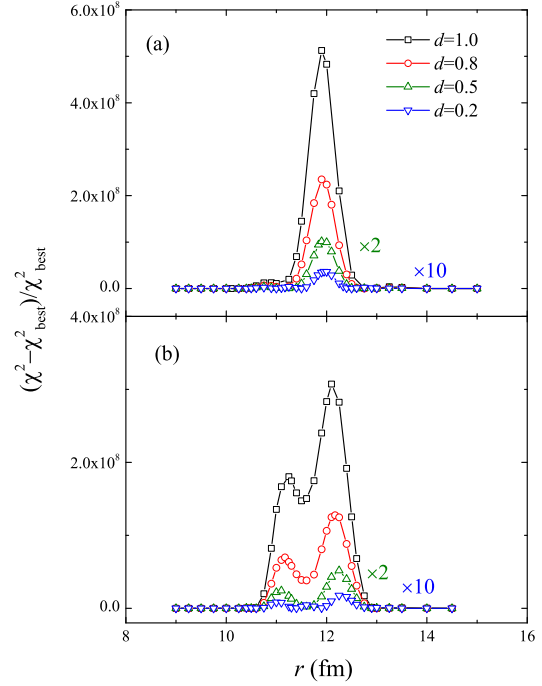


Fig. 3. (Color online) The sensitivity functions for the real part (a) and imaginary part (b) potentials with different  $d$  values. The “ $\times 10$ ” symbols mean the corresponding results with the same color are multiplied by 10 for the convenience of comparison. There are same meanings for times signs in the following figures. The curves are used to guide the eyes.

The notch width  $a'$  was set at 0.2, 0.1, 0.05 and 0.01 fm, respectively, and the corresponding sensitivity functions are shown in Fig. 4. It can be seen that a wider perturbation introduces a stronger influence, leading to a larger relative  $\chi^2$  value. However, the original distinct double-peaked structure in the imaginary part disappears when a large value of  $a'$  was adopted, replaced by one broad peak containing the gross information of the radial sensitivity. On the contrary, when  $a' = 0.01$  fm, which is equal to the integration step size  $dr$ , three peaks emerge in the sensitivity function of the imaginary part potential. As mentioned in Ref. [5], problems may be arising when  $a'$  becomes comparable to the  $dr$ . Based on the above discussions, we argue that a smaller  $a'$  is benefit to extract the fine information on the sensitivity of the radial potential, but not too close to the integration step. The  $a'$  value of 0.05 fm, about 5 times of the integration step  $dr$ , is adopted afterward.

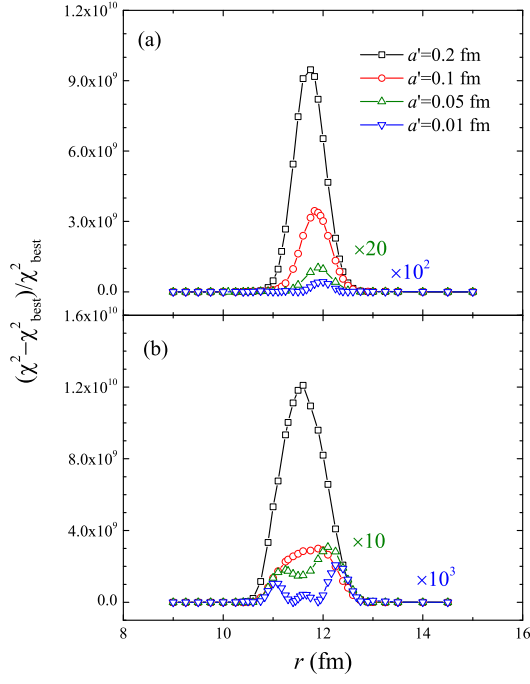


Fig. 4. (Color online) The same as Fig. 3, but with different perturbation width  $a'$  values.

### 3.2.2 OMP parameters

With the fixed perturbation parameters, further investigations were performed on the OMP parameters. First, the ideal angular distribution was fitted with  $r_{0i}$  fixed at 1.20, 1.25 and 1.30 fm, respectively, and results are shown in Fig. 5. Second, the fitting procedure was repeated but with  $a_i$  fixed at 0.60, 0.65 and 0.70 fm, respectively, and results are shown in Fig. 6. One can see that relative  $\chi^2$  values between the main (major) peaks and tiny (minor) peaks for the real (imaginary) part vary obviously with the  $r_{0i}$  and  $a_i$ . However, nearly same sensitive regions were determined by those OMP parameter sets, although the relative sensitivity differed from each other. Therefore, it can be concluded that the sensitive region determined by the notch technique is nearly model-independent.

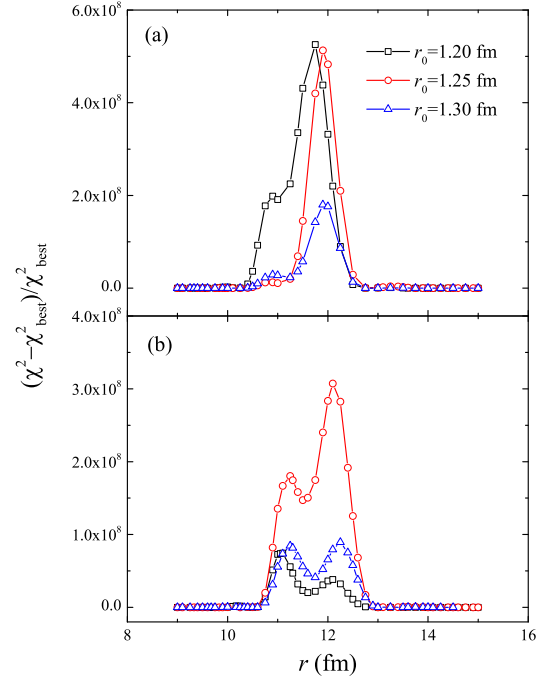


Fig. 5. (Color online) The sensitivity functions for the real part (a) and imaginary part (b) potentials with different OMP parameters derived with fixed  $r_{0i}$ . The curves are used to guide the eyes.

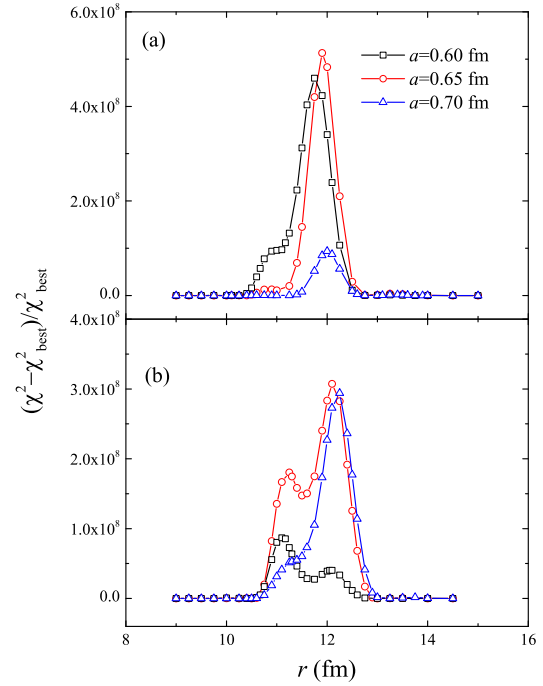


Fig. 6. (Color online) The same as Fig. 5, but with the OMP derived with fixed  $a_i$ .

### 3.3 dependence on the experimental data

After the investigation of the model dependence, a further sensitivity test on the experimental data was performed, to assess the influence arising from the quality

of the data set, and provide some guidance on the experimental measurements.

### 3.3.1 angle interval

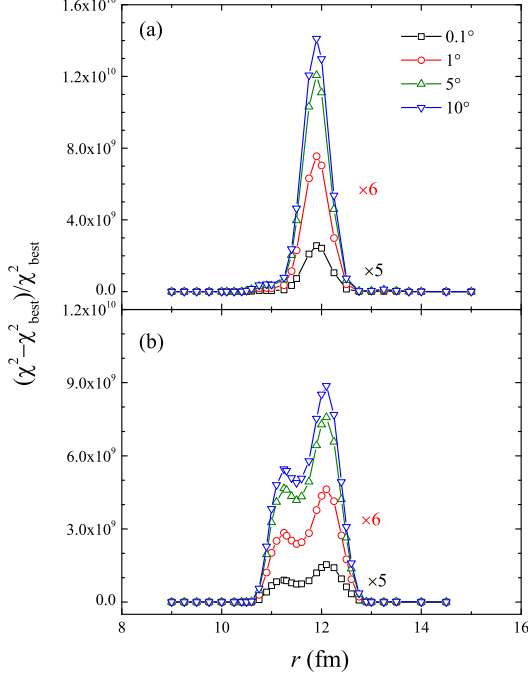


Fig. 7. Color online) The sensitivity functions for the real part (a) and imaginary part (b) potentials for experimental data set with different  $\theta_{\text{int}}$ . The curves are used to guide the eyes.

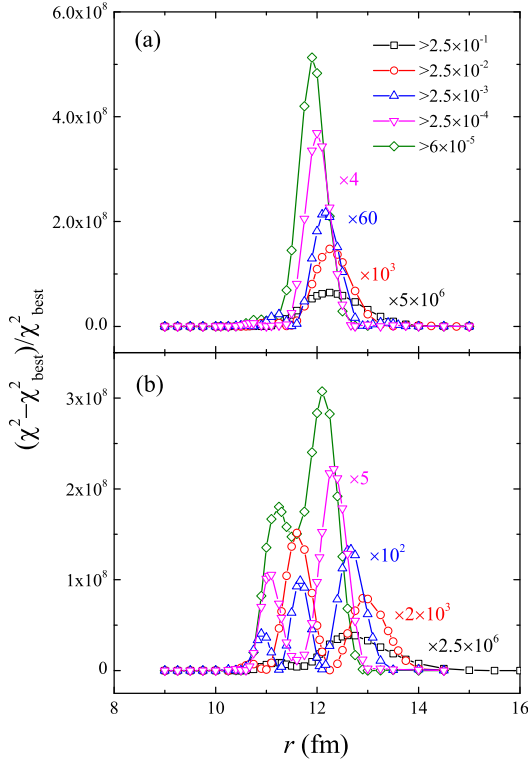


Fig. 8. (Color online) The same with Fig. 7, but with different  $d\sigma_{\text{el}}/d\sigma_{\text{Ru}}$  extensions.

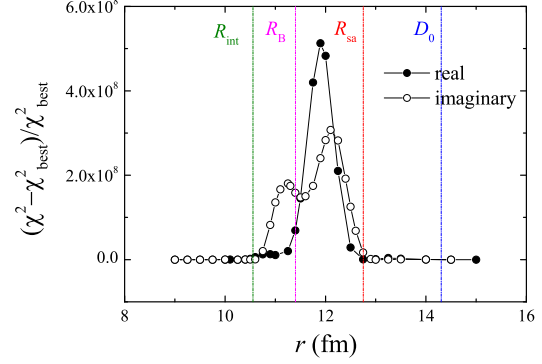


Fig. 9. (Color online) The sensitivity functions of the real (full circle) and imaginary (hollow circle) parts with the data range down to  $d\sigma_{\text{el}}/d\sigma_{\text{Ru}} = 6.0 \times 10^{-5}$ . The interaction radius  $R_{\text{int}}$ , Coulomb barrier radius  $R_{\text{B}}$ , strong absorption radius  $R_{\text{sa}}$ , and the distance  $D_0$  are shown by vertical lines. See the text for detail.

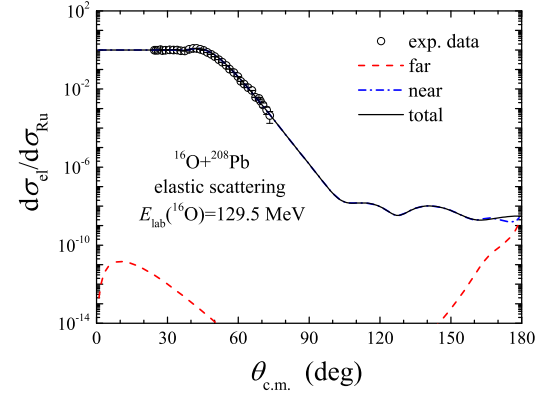


Fig. 10. (Color online) The elastic angular distribution of  $^{16}\text{O} + ^{208}\text{Pb}$  at  $E_{\text{lab}}(^{16}\text{O}) = 129.5$  MeV. Open circles represent the experimental data. Best-fit result is shown by the solid curve. Decomposition of the far- and near-side are also shown by the dashed and dot-dashed curves, respectively.

It can be imagined that a fine angle interval may be useful in determining a reliable OMP parameter set but it is time consuming, especially for the RIB experiment. In order to check its influence on the sensitive region, different angle intervals  $\theta_{\text{int}}$ , i.e.  $\theta_{\text{int}} = 0.1^\circ, 1^\circ, 5^\circ$  and  $10^\circ$  were adopted to the ideal data set. The corresponding sensitivity functions are shown in Fig. 7. It can be seen that bigger  $\theta_{\text{int}}$  introduces a larger  $\chi^2$  value. There are no obvious changes in the structures of the sensitivity functions for both the real and imaginary parts. It demonstrates that on the premise of large angle-region as well as good statistics, the sensitive region can be determined accurately even by a few experimental data

points. This conclusion is important to the elastic scattering measurements with RIBs, whose angular distributions usually have a few points due to the limits of the intensity and quality of the available RIBs [15, 16]. However, it should be kept in mind this indication is only available for the heavy target system, whose angular distribution of elastic scattering is almost structureless. When refers to the light nuclear system, whose elastic scattering angular distribution presents strong interference pattern, a fine measurement is necessary to describe the detailed structure of the angular distribution.

### 3.3.2 angle region

In principal, the wider angle region is measured, the more constraint on the OMP parameters can be achieved. However, it is hard to extend the experimental data to the large angle where the cross section become very low for the elastic scattering, especially at high energies. From the physics point of view, data at the back angle may provide more information on the inner potential. In order to inspect the influences of angle region measured, the ideal data were divided into five sets: the first set contains the data down to  $d\sigma_{el}/d\sigma_{Ru} = 0.25$  at the grazing angle, corresponding to the one-half of the transmission coefficient; the second set contains the data down to  $d\sigma_{el}/d\sigma_{Ru} = 0.025$ , etc., until the fifth set, which contains all the data points cut off at  $\theta_{c.m.} = 80^\circ$ , where  $d\sigma_{el}/d\sigma_{Ru} = 6.0 \times 10^{-5}$ . Results of sensitivity test for each data set are shown in Fig. 8. Distinct peaked structures are observed for both the real and imaginary potential parts. In order to evaluate quantitatively the influences of the data region measured, the main peak of the real part and major peak of the imaginary part were fitted by a Gaussian function, respectively. Values of the center position as well as its sigma width are listed in Table 1.

Table 1. The center(sigma) values of the peaks observed in Fig. 8. The real and imaginary correspond to the main peak of the real part and the major peak of the imaginary part, respectively. The value of the center is in the unit of fm.

data range	real	imaginary
$> 2.5 \times 10^{-1}$	12.31(0.56)	12.76(0.57)
$> 2.5 \times 10^{-2}$	12.29(0.34)	13.02(0.34)
$> 2.5 \times 10^{-3}$	12.17(0.25)	12.68(0.25)
$> 2.5 \times 10^{-4}$	12.01(0.23)	12.33(0.25)
$> 6.0 \times 10^{-5}$	11.91(0.25)	12.10(0.31)

For the first data set only containing the data with  $d\sigma_{el}/d\sigma_{Ru} > 0.25$ , the nuclear force just begins to take effect, thus it is difficult to obtain the accurate information of the nuclear potential, so a very broad peak presents. As we extended the data to larger angles, the effects of the nuclear force begin to increase, and more detailed information can be extracted. Meanwhile both the main peak of the real part and the major peak of the

imaginary part systematically move into the inner with angle going backward. However, considering the peripheral nature of elastic scattering, the inner potential can not be probed when the distance is short than a certain value.

Moreover, one can find that the lower cross section of the elastic scattering is measured, the larger relative  $\chi^2$  value will be got. The relative  $\chi^2$  value of the fifth set is  $10^7$  times larger than that of the first set. As mentioned above, the value of relative  $\chi^2$  represents the sensitivity degree of the OMP parameters on the elastic scattering data. Such a large relative  $\chi^2$  value demonstrates that a well adequate constraint can be achieved for the OMP parameters within the sensitive region when the measurement reaches to a very low cross section.

### 3.4 discussion

The ideal test provides a solid foundation for the application of the notch technique. With the appropriate parameters of the notch and OMP, the physical meanings of sensitivity peaks can be understood. In order to demonstrate clearly, several available radii and distance, e.g. the radius of the interaction potential  $R_{int}$ , Coulomb barrier radius  $R_B$ , strong absorption radius  $R_{sa}$ , as well as the distance  $D_0$  where the nuclear force begins to take effect, are labeled in Fig. 9 by vertical lines. The  $R_{sa}$  is the radius where the observed cross section has fallen to one-fourth of the Rutherford value; and  $D_0$  corresponds to the distance of  $d\sigma_{el}/d\sigma_{Ru} = 0.98$ . One can find that even for data down to  $d\sigma_{el}/d\sigma_{Ru} = 6.0 \times 10^{-5}$ , the main sensitivity regions located around 12.0 fm, far larger than the  $R_{int}$ , 10.56 fm, demonstrating that the OMPs determined by the elastic scattering are only sensitive to surface regions. And as mentioned in Ref. [6], because of the strong absorption, it seems unlikely that much light can be shed on the behavior of the real potential in the deep interior region with measurements of heavy-target system elastic scattering.

For the imaginary part, two distinct peaks are observed. The major one lies around the  $R_{sa}$ , corresponding to the surface absorption process; the minor peak locates around the  $R_B$ , which should be responsible for the volume absorption, i.e. the capture reaction process. While for the real part, the main peak locating near the  $R_{sa}$ , followed by a tiny inner peak, which lies inside of the  $R_B$ . Both of the two real-part peaks locate inside of the corresponding imaginary ones. The main peak of the real part is arising from the direct scattering process. The origin of the tiny peak was thought to be associated with the far-side interference effect [5, 8]. In order to check the reliability of this explanation, the decomposition of the far- and near-side scattering was performed with the method developed in Ref. [17], and the result is shown in Fig. 10. One can find that the far-side scatter-

ing is almost negligible for the whole angle range, indicating that the tiny peak should not be originated from the interference between the far- and near-side components. Considering that the location of the tiny peak is inside of  $R_B$ , we believe this peak should be the result of the resonance scattering, where the compound nucleus has been formed.

## 4 Summary and conclusions

The sensitivities of the notch technique on the parameters of the perturbation and OMP, as well as the experimental data were investigated in the present work. Through the ideal test we can draw the conclusions as below: 1) a sufficient large reduced fraction  $d$  can help to obtain accurate information of the sensitive region, and  $d=1.0$  is the adopted value; 2) the width of the perturbation  $a'$  should be several times of the integration step  $dr$ , an inappropriate large or small value of  $a'$  will lead to a spurious result; 3) the notch technique is almost independent on the OMP parameters; 4) for the heavy-target nuclear system, on the premise of large angle-region as well as good statistics measurement, there is no need of a great deal of experimental data points to ensure the reliability of the sensitive region extracted. This may aid in optimizing the setup of elastic scattering measurement, especially for the experiments with RIBs; 5) the relative inner information of the nuclear potential can be derived when measurement extended to a lower elastic scattering cross section. However, the deep interior region of the nuclear potential is still invisible through

the elastic scattering measurement due to the effect of strong absorption.

With these detailed investigations of the notch technique, we can further apply this method to the researches on the radial sensitivities of both tightly- and weakly-bound nuclear systems, which are essential issues in the studies of the OMP.

## References

- 1 M. E. Brandan and G. R. Satchler, Phys. Rep. **285**, 143 1997.
- 2 N. Keeley, N. Alamanos, K. W. Kemper, and K. Rusek, Prog. Part. Nucl. Phys. **63**, 396 2009.
- 3 N. Keeley, R. Raabe, N. Alamanos, and J. L. Sida, Prog. Part. Nucl. Phys. **59**, 579 2007.
- 4 G. Igo, Phys. Rev. Lett. **1**, 72 1958.
- 5 J. G. Cramer and R. M. DeVries, Phys. Rev. C **22**, 91 1980.
- 6 P. J. Moffa, C. B. Dover, and J. P. Vary, Phys. Rev. C **13**, 147 1976.
- 7 C. J. Lin, J. C. Xu, H. Q. Zhang *et al.*, Phys. Rev. C **63**, 064606 2001.
- 8 D. Roubos, A. Pakou, N. Alamanos, and K. Rusek, Phys. Rev. C **73**, 051603(R) 2006.
- 9 M. H. Macfarlane and S. C. Pieper, Phys. Lett. B **103**, 169 1981.
- 10 M. Biswas, Phys. Rev. C **77**, 017602 2008.
- 11 F. Michel, J. Albinski, P. Belery *et al.*, Phys. Rev. C **28**, 1904 1983.
- 12 J. D. Brown, E. Lau and S. Roman, J. Phys. G: Nucl. Phys. **10**, 1391 1984.
- 13 I. J. Thompson, Comp. Phys. Rep. **7**, 167 1988.
- 14 J. B. Ball, C. B. Fulmer, E. E. Gross *et al.*, Nucl. Phys. A **252**, 208 1975.
- 15 E. F. Aguilera, J. J. Kolata, F. D. Becchetti *et al.*, Phys. Rev. C **63**, 061603(R) 2001.
- 16 E. F. Aguilera, E. Martinez-Quiroz, D. Lizcano *et al.*, Phys. Rev. C **79**, 021601(R) 2009.
- 17 R. Anni, J. N. L. Connor, and C. Noli, Phys. Rev. C **66**, 044610 2002.